BULETINUL INSTITUTULUI POLITEHNIC DIN IAŞI
Publicat de
Universitatea Tehnică „Gheorghe Asachi” din Iaşi
Volumul 62 (66), Numărul 3, 2016
Secţia
CONSTRUCŢII DE MAŞINI

# EXPERIMENTAL INVESTIGATION OF FREE RESPONSE ON A CANTILEVER BEAM (FIRST FLEXURAL VIBRATION MODE)

BY

**MIHĂIȚĂ HORODINCĂ***

"Gheorghe Asachi" Technical University of Iaşi,
Faculty of Machines Manufacturing and Industrial Management

Received: October 3, 2016
Accepted for publication: October 19, 2016

**Abstract.** This paper investigates the free response of first flexural vibration mode on a cantilever beam, mirrored in the signal delivered by a PZT piezoelectric plate transducer bonded near the fixed end, used as sensor. Despite the generally accepted theoretical model (as viscous damped free response with constant damping ratio and undamped angular frequency) it is experimentally proved that the real response is characterized by a relatively important variation of damping ratio and undamped angular frequency values, both depending by the amplitude of vibration. The investigation was done on a simple setup, by computer aided processing of the signal delivered by sensor.

**Keywords:** vibration; free response; cantilever beam; signal processing.

## 1. Introduction

A cantilever beam (as a simple example of vibratory mechanical system) is often used to introduce and illustrate different concepts in passive and active dynamics (Jassim *et al.*, 2013; Guan *et al.*, 2016). Frequently this free response on first flexural mode reveals the properties of the environment (Kramer *et al*., 2013) or materials (Paimushin *et al*., 2015).

*Corresponding author; *e-mail*: horodinca@tuiasi.ro

If the cantilever beam is placed in horizontal position, the free vibration on this mode is generally described as the movement $x(t)$ of the free end in vertical direction. In order to describe this movement $x$, [mm] related to time $t$, [s], the theoretical model of free viscous damped response of a single degree of freedom (spring-mass-damper) system (with constant values for damping ratio $\xi$, [] and undamped angular frequency of vibration $\omega_0$, [rad/s]) is generally used (Kelly, 2000), according to Eq. (1).

$$x(t) = a \cdot e^{-\xi \cdot \omega_0 \cdot t} \cdot \sin(\sqrt{1-\xi^2} \cdot \omega_0 \cdot t + \varphi) \tag{1}$$

where: $a$, [mm] is the maximum amplitude and $\varphi$, [rad] is the phase at $t$ = 0.

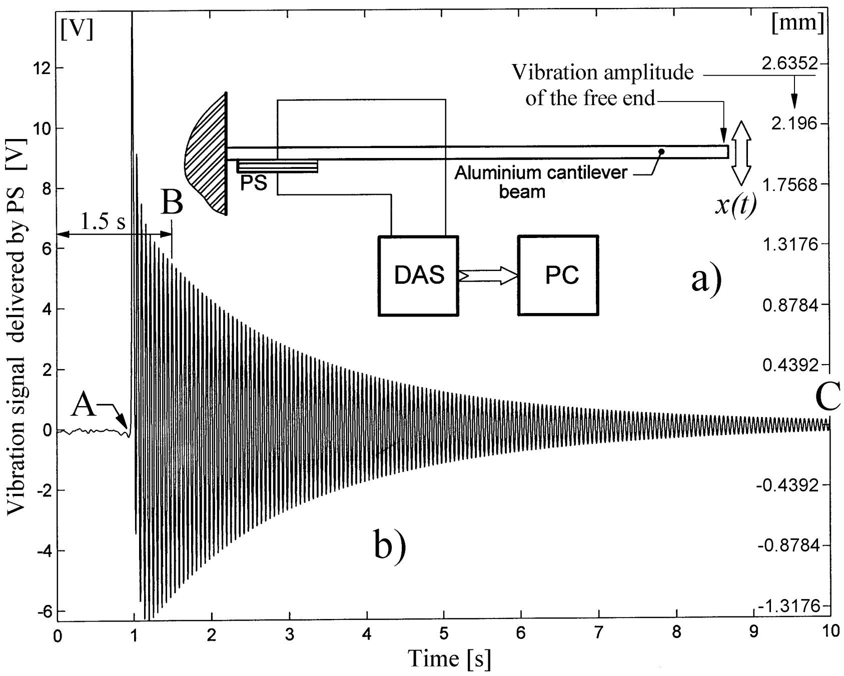


Fig. 1 – *a*) Experimental setup; *b*) Free response mirrored in the signal delivered by a PZT piezoelectric sensor (PS) with laminar rectangle design.

The research results disclosed herein proves by computer aided signal processing that -for relatively high values of vibration amplitude- this model is not accurate, the vibration parameters invoked above ($\xi$ and $\omega_0$) are not constant and they heavily depend on vibration amplitude value (especially the damping ratio).

These results might be important for certain applications and it is expected to be useful for future approaches in dynamics.

## 2. Experimental Setup

The experimental setup is described in Fig. 1*a*. It consists of an aluminium cantilever beam (300x25x2 $mm^3$) with a PZT piezoelectric transducer PS (used as sensor, with laminar rectangular design, 40x25x0.5 $mm^3$, Sensor Tech BM 500 type, $d_{31}$ polarization, with $d_{31} = -175 \cdot 10^{-12}$ m/V) bonded on the close proximity of the rigidly fixed end of the cantilever beam.

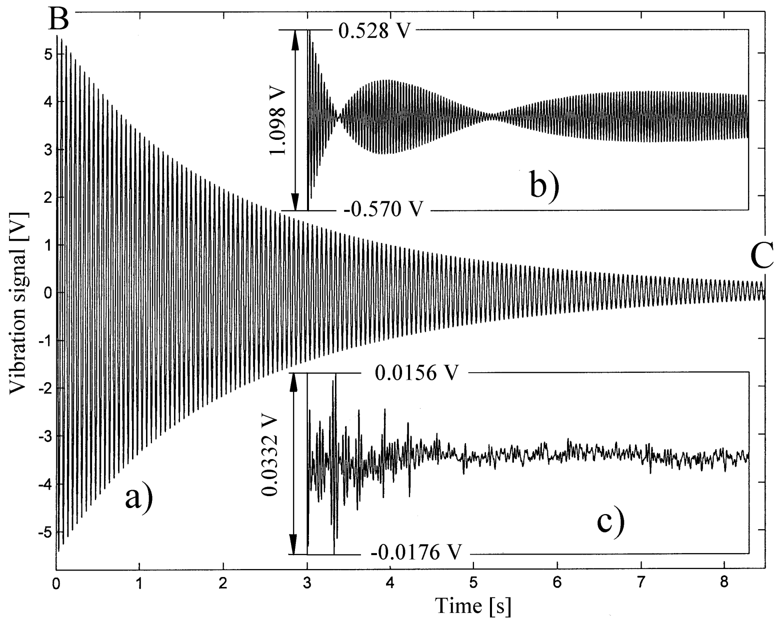


Fig. 2 – *a*) A part of signal from Fig. 1*b* used for fitting; *b*) The residual of a single fitting ($t_B < t < t_C$ ); *c*) The residual of fitting on intervals $(k\text{-}1)\cdot\Delta t < t_i <= k\cdot\Delta t$.

Due to th**e** flexural vibration $x(t)$ related with the free response (underdamped vibrations) on the first flexural mode of the cantilever beam, (which produces mechanical strain in the area where the sensor is placed (Horodincă, 2013) and the direct piezoelectric effect, the sensor generates a voltage $u(t) = C \cdot x(t)$, with $C$ = 4.553 V/mm (a value supposed to be constant).

## 3. Signal Processing Technique (I)

This voltage is acquired in numerical format using a data acquisition system (DAS on Fig. 1*a*, with a 4424 PicoScope oscilloscope) and analyzed with a personal computer PC. Fig. 1*b* present the evolution of this voltage before and after the free response occurs (in A, manually excited). As Fig. 1*b* clearly indicates, the free response is totally mirrored in the evolution of this voltage. Assuming that the Eq. (1) describes $x(t)$ evolution between the moments depicted with B ($t_B$) and C ($t_C$) then:

$$u(t) = C \cdot x(t) = A \cdot e^{-\xi \cdot \omega_0 \cdot t} \cdot \sin(\sqrt{1-\xi^2} \cdot \omega_0 \cdot t + \varphi) \qquad (2)$$

where: $t_B < t < t_C$ and $A = C \cdot a$, [V] is the maximum amplitude of the voltage.

The voltage between B and C -from Fig. 1*b*- is also drawn in Fig. 2*a*, considering $t_B = 0$ and $t_C = 8.5$ s.

The best way to check if the theoretical model from Eq. (2) correctly describes the experimental free response signal from Fig. 2*a* is the computer aided numerical fitting. The residual of curve fitting indicates the accuracy of the model. The best fitting means to find the appropriate values for the parameters ($A$, $\xi$, $\omega_0$ and $\varphi$) involved in Eq. (2) in order to obtain a theoretical voltage evolution $u^t(t)$ which fits with maximum accuracy on the experimental voltage $u^e(t)$.

A computer aided fitting technique based on the minimal value of the cumulative error $\varepsilon$, [V] - depicted in Eq. (3) - was developed in order to find the best approximation for the parameters $A$, $\xi$, $\omega_0$ and $\varphi$ involved in $u^t(t)$ definition.

$$\varepsilon = \sum_{t_j = t_B}^{t_j = t_C} \left| u^e(t_j) - u^t(t_j) \right| = \min \qquad (3)$$

With $\varepsilon = 0$ (a hypothetical situation) the theoretical and experimental voltages totally fit. An appropriate range and an increment of variation for each parameter were established. The set of four values of these parameters which produce a minimal cumulative error $\varepsilon$ describes - according to Eq. (2) - the best fitting curve.

## 4. Experimental Results (I)

According to the procedure previously described, the experimental signal from Fig. 2*a* was numerically fitted. The values of parameters involved in Eq. (2) founds by fitting are written bellow in Table 1:

**Table 1**

*Values of Fitting Parameters (a Single Fitting, for $t_B < t < t_C$)*

| $A$, [V] | $\xi$, []·100 | $\omega_0$, [rad/s] | $\varphi$, [rad] |
|---|---|---|---|
| 5.2580 | 0.3792 | 112.9871 | 1.4196 |

Fig. 2*b* presents the evolution of the residual ($u^e(t_j)$- $u^t(t_j)$ with $t_B < t_j < t_C$). It is clear that the theoretical curve doesn't fit well the experimental evolution. Definitely this does not happen because of the fitting technique. The only available hypothesis is that the damping ratio and undamped angular frequency on experimental signal are not constant related to time. It is obvious that the beating phenomenon on Fig. 2*b* indicates certainly a variable undamped angular frequency.

With a good approximation it can be considered that the model depicted in Eq. (2) is available only for small intervals of time (*e.g.* $\Delta t$ = 0.5 s). The signal fitting has been made once again on each interval (with $(k\text{-}1)\cdot\Delta t < t_i <= k\ \Delta t$), with the values found for fitting parameters written in Table 2. Before fitting, the evolution $u^e(t_j)$ on each interval was moved in origin on the abscissa.

**Table 2**

*Values of Fitting Parameters* (*Fitting on Intervals* $(k\text{-}1)\ \Delta t < t_i <= k\cdot\Delta t$)

| $k$ | $A_k$, [V] | $\xi_k$, []·100 | $\omega_{0k}$, [rad/s] | $\varphi_k$, [rad] |
|---|---|---|---|---|
| 1 | 5.4757 | 0.4421 | 112.8134 | 1.5193 |
| 2 | 4.2637 | 0.4291 | 112.8692 | 1.4036 |
| 3 | 3.3522 | 0.3978 | 112.9239 | 1.3173 |
| 4 | 2.6813 | 0.3792 | 112.9726 | 1.2601 |
| 5 | 2.1656 | 0.3621 | 113.0080 | 1.2254 |
| 6 | 1.7644 | 0.3498 | 113.0403 | 1.2082 |
| 7 | 1.4467 | 0.3480 | 113.0649 | 1.2060 |
| 8 | 1.1865 | 0.3373 | 113.0864 | 1.2168 |
| 9 | 0.9814 | 0.3384 | 113.1050 | 1.2401 |
| 10 | 0.8121 | 0.3321 | 113.1154 | 1.2717 |
| 11 | 0.6720 | 0.3237 | 113.1295 | 1.3096 |
| 12 | 0.5592 | 0.3201 | 113.1396 | 1.3518 |
| 13 | 0.4655 | 0.3154 | 113.1499 | 1.4034 |
| 14 | 0.3877 | 0.3107 | 113.1583 | 1.4563 |
| 15 | 0.3237 | 0.3102 | 113.1663 | 1.5113 |
| 16 | 0.2696 | 0.3100 | 113.1703 | 1.5722 |
| 17 | 0.2253 | 0.3113 | 113.1660 | 1.6423 |

This technique of numerical fitting produces much better results as clearly is proved by the evolution of the residual given in Fig. 2*c*. Here the maximum peak to peak magnitude is 33 times less than in Fig. 2*b*. At the end of the evolution the residual is dominated by mechanical and electrical noise (vibrations in the environment and electromagnetic fields). At the beginning, the residual is possible dominated by some other excited vibration modes (poorly described by the sensor PS).

As expected, the damping ratio value is not constant, it has a relatively important variation: it decreases with the decreasing of vibration amplitude (as it is also graphically depicted in Fig. 3), while the undamped angular frequency increases slowly (as it is also graphically depicted in Fig. 4).

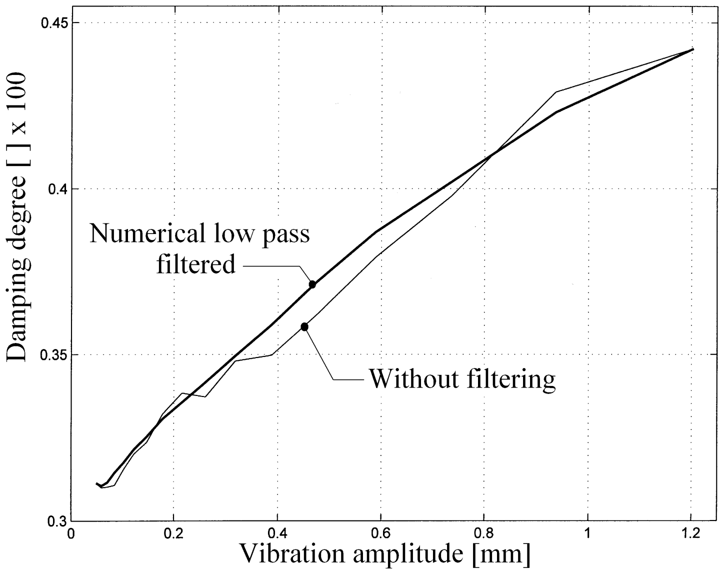


Fig. 3 – Evolution of damping ratio $\xi_k$ (x100) related to vibration amplitude $a_k=A_k/C$.

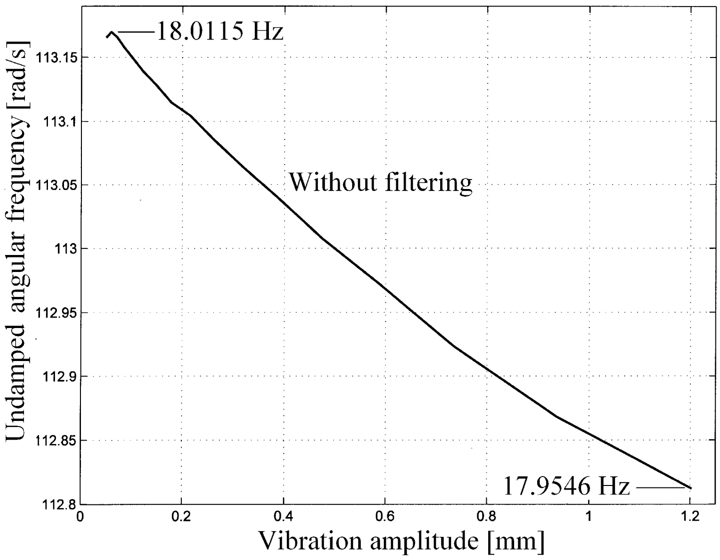


Fig. 4 – Evolution of undamped angular frequency $\omega_{0k}$ related to vibration amplitude $a_k=A_k/C$.

This means that the model proposed in Eq. (1) and Eq. (2) should be revised if it is used for large intervals of time. This dependence of damping ratio by vibration amplitude seems to be an important item useful in dynamics of cantilever beams.

For example, related with the researches exposed in (Horodincă, 2013), this result explains why when a vibratory mechanical system is actively supplied with positive mechanical modal power (which produces negative synthetic damping on first flexural mode of vibration) beyond of the stability limit, the amplitude of vibrations increases (and the absorbed modal power too) up to a certain limit depending by synthetic damping value. At this limit, the passive (positive!) damping in system (which increases with the increasing of amplitude) completely cancel the synthetic damping (negative, constant), the total damping becomes zero. The actuation input power flow becomes equal with the output (passive) power flow.

## 5. Signal Processing Technique (II)

Generally speaking the first signal processing technique exposed before (by curve fitting) has an important disadvantage: it takes time to apply. There is a simpler way to find out the evolution of $\xi$ and $\omega_0$ related by vibration amplitude.

On the evolution depicted in Fig. 2*a* let be $a_i$ and $a_{i+1}$ two consecutive current values of the signal amplitude (each one achieved at the instant times $t_i$ and $t_{i+1}$ respectively), according to Fig. 5*a*. These amplitudes are written with the considerations from Eq. (2) as follows:

$$a_i = \frac{A}{C} \cdot e^{-\xi_i \cdot \omega_{0i} \cdot t_i}, \qquad a_{i+1} = \frac{A}{C} \cdot e^{-\xi_{i+1} \cdot \omega_{0(i+1)} \cdot t_{i+1}} \tag{4}$$

where: $t_{i+1}$-$t_i$ = $T_j$ is the value of current period of the signal, and $\omega_{0i}$ is the current value of the undamped angular frequency, related by the current value of damping ration $\xi_i$ and damped angular frequency $\omega = 2 \cdot \pi / T_j$ (Kelly, 2000) by equation:

$$\omega_{0i} = \frac{2 \cdot \pi}{T_j} \cdot \frac{1}{\sqrt{1 - \xi_i^2}} \tag{5}$$

In order to simplify this approach, let consider that $\xi_i = \xi_{i+1}$ and $\omega_{0i} = \omega_{0(i+1)}$. Let be $\delta_i$ the current value of the logarithmic decrement defined as:

$$\delta_i = \ln(\frac{a_i}{a_{i+1}}) = \ln(e^{\xi_i \cdot \omega_{0i} \cdot T_j}) = \xi_i \cdot \omega_{0i} \cdot T_j \tag{6}$$

These two last equations allow the calculus of current values for $\omega_{0i}$ and $\xi_i$, considering that $a_i$, $a_{i+1}$ and $T_j$ are previously determined by computer aided analysis of the signal from Fig. 2*a*, see the symbolic approach from Fig. 5*a* . If we assume that $n = 2\cdot\pi/T_j$, $m = \delta_i/T_j$ and $h = m/n$, then $\xi_i$ is given by:

$$\xi_i = \frac{h}{\sqrt{1+h^2}} \tag{7}$$

With this result, the Eq. (5) allows the calculus for $\omega_{0i}$.

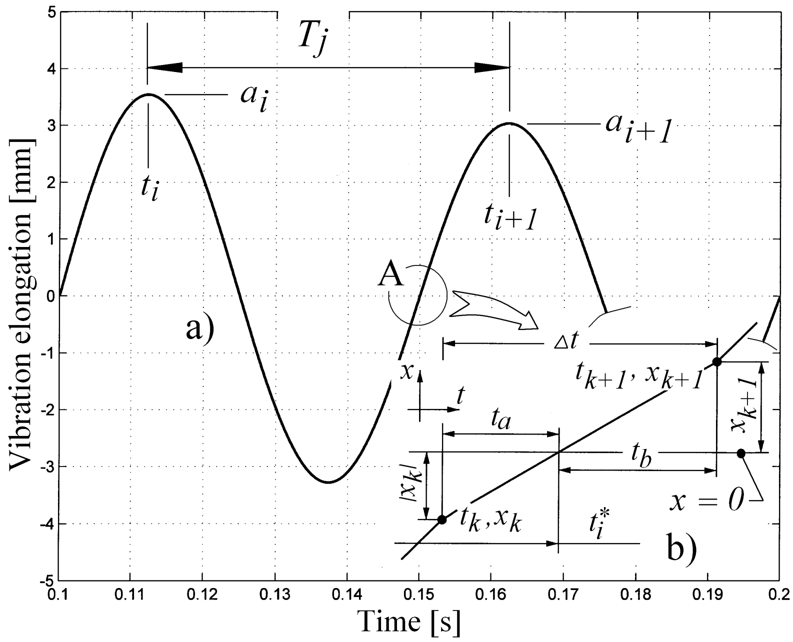


Fig. 5 – *a*) A symbolic approach for determination of amplitudes $a_i$, $a_{i+1}$ and period $T_j$; *b*) Some considerations related to exact calculus of period $T_j$.

It is important to highlight that ($t_i$, $a_i$) and ($t_{i+1}$, $a_{i+1}$) are two signal samples. The values of amplitudes and instant times (and consequently of current period $T_j$ of the signal) are more accurately determined if smaller sampling period (or a bigger sampling rate) is used. Here the sampling rate is 10,000 $s^{-1}$ (or 278 samples per signal period, approximately). The accuracy of amplitudes is not a critical item, whereas are involved mainly in the definition of damping ratio (which has an important variation as was pointed in Fig. 3). But the accuracy of current period $T_j$ - whereas is involved mainly in the definition of undamped angular frequency (with a very small variation as was already pointed in Fig. 4) - is very important.

For this reason, the highest accuracy possible technique for determining the value of $T_j$ was developed according to Fig. 5*b*. The numerical evolution of the vibration elongation $x(t)$ is graphically depicted as a succession of points (samples) connected by line segments. Let be $(t_k, x_k)$ and $(t_{k+1}, x_{k+1})$ the coordinates of two neighbouring points placed below and above the abscissa axis $t = 0$ (generally with $x_k < 0$ and $x_{k+1} > 0$). Here $t_{k+1}$-$t_k$ = $\Delta t$ is the sampling period already introduced before. Let be $t_i^* = t_k+t_a$ the abscissa value for the point of intersection of segment line with abscissa axis. There are two similar triangles on Fig. 5*b*, so $t_a$ and $t_i^*$ can be described as:

$$t_a = \frac{|x_k|}{|x_k| + x_{k+1}} \cdot \Delta t \qquad t_i^* = t_k + \frac{|x_k|}{|x_k| + x_{k+1}} \cdot \Delta t \tag{8}$$

A similar description can be done for next intersection $t_{i+1}^*$ of $x(t)$ evolution with abscissa axis, so the exact value of current period is given by:

$$T_j = t_{i+1}^* - t_i^* \tag{9}$$

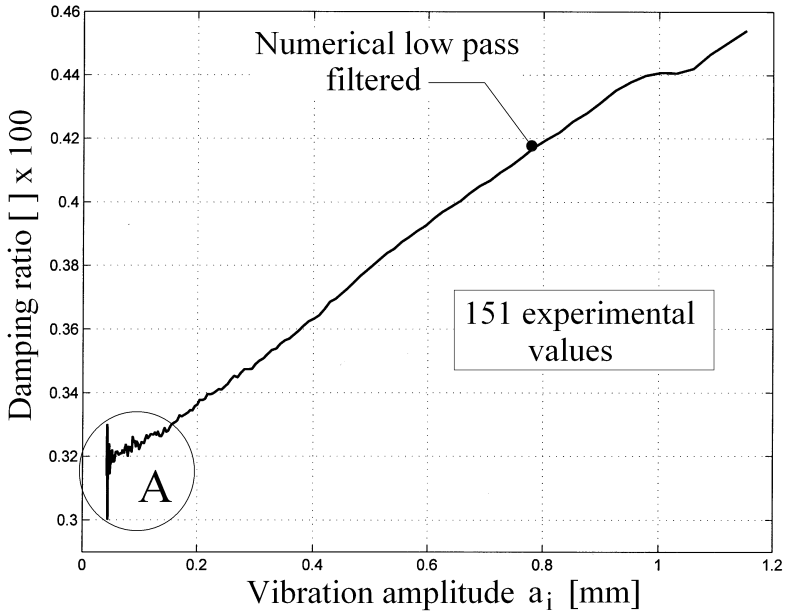


Fig. 6 – Evolution of damping ratio $\xi_i$ (x100) versus vibration amplitude $a_i$.

In this approach, Eq. (8) is available also if $x_k = 0$ or $x_{k+1} = 0$. This calculation method is also available for an accurate calculus of period (and frequency as well) for all periodic experimental signals numerically described.

## 6. Experimental Results (II)

With these considerations, the evolution of damping ratio $\xi_i$ versus amplitude $a_i$ was experimentally determined - Eq. (7) - as it is graphically depicted in Fig. 6.

The evolution is quite similar with those already given in Fig. 3. But generally speaking it is more accurate and contains more experimental points (151 values). In the area marked with A (here and in Fig. 7 as well) the accuracy is bad because of the measurement noise (electrical and mechanical). This noise becomes important related with vibration amplitude value (which has a low level here).

Fig. 7 shows the evolution of undamped angular frequency $\omega_{0i}$ versus vibration amplitude $a_i$ based on Eq. (5).

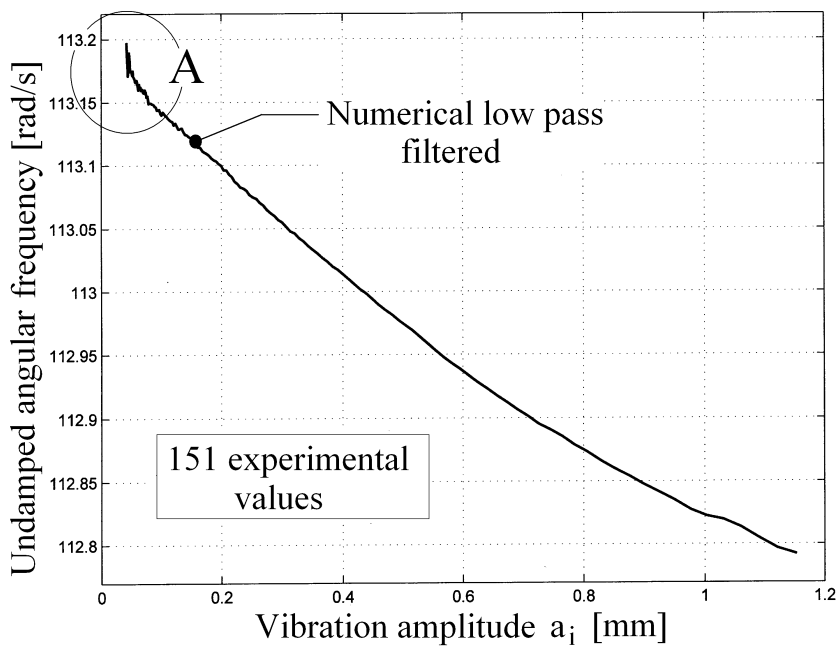


Fig. 7 – Evolution of undamped angular frequency $\omega_{0i}$ versus vibration amplitude $a_i$.

Here also a comparison with Fig. 4 proves that this new signal processing technique is correct.

Besides accuracy, this technique has also the advantage of a facile employment. The evolutions from Figs. 6 and 7 can be numerically fitted in order to find out the analytical form for $\xi_i = \xi_i(a_i)$ and $\omega_{0i} = \omega_{0i}(a_i)$ useful for different theoretical and experimental approaches in mechanical dynamics.

## 7. Conclusions

The paper proves in experimentally terms that the free response on first flexural vibration mode of a cantilever beam is characterized - despite the generally accepted theoretical model (the free response of an underdamped spring-mass-damper system) - by a relative significant variation of damping ratio $\xi$ (according to Figs. 3 and 6) and a relatively slight variation of the undamped angular frequency $\omega_0$ (according to Figs. 4 and 7), both related with vibration amplitude evolution.

A simple setup based on a cantilever beam with a PZT sensor, a data acquisition system (with numerical oscilloscope) and a personal computer was used, as is revealed in Fig. 1*a*). It is presumed that the signal delivered by sensor is proportional with the vibration elongation of the free end of the cantilever beam (on first vibration mode).

The evolutions of $\xi$ and $\omega_0$ were evaluated using two different computer processing techniques for the signal delivered by the PZT sensor placed in the proximity of the fixed end of the cantilever beam during the free response of the cantilever beam.

The first technique (relatively accurate) is based on numerically fitting of the experimental signal divided in sequences with short durations of time (0.5 s), while the second technique (more accurate and faster) is based on numerical processing of the evolution of amplitude and period of the signal. Both techniques were conceived and developed by author.

These results are interesting for scientific research in dynamics (https://www.mathworks.com/help/pde/). For example, an ambiguous item from a previous research (Horodincă, 2013) is clarified here: the increasing of passive damping ratio when the amplitude of vibration increases explain why if a negative synthetic modal damping is generated (by positive active modal mechanical power flow in a system with positive velocity-force feedback) the amplitude of vibration increases until the passive (positive) damping completely cancel the synthetic (negative) damping. If the total modal damping (synthetic and passive) is negative, the system becomes unstable, it starts vibrating.

In the near future the theoretical and experimental approach presented here (related by second processing technique of the signal) will be applied on the same setup, but using as strain sensor for flexural vibration a Wheatstone bridge with strain gauges placed also by bonding near the fixed end of the cantilever, collocated with the PZT sensor. A previous result of research (Horodincă, 2013) indicates that between the strain (as it is described by PZT sensor with an electrical voltage evolution) and vibration $x(t)$ at free end in cantilever beam (due to the flexural vibration on the first mode) exists a shift of phase (with a presumed average value of $14^o$). A future research should establish a measurement and compensation technique in order to eliminate this phase shifting when the PZT transducers are used as sensor and actuator in a close loop feedback control system. Otherwise a feedback with a pure proportional control law acts as a proportional-derivative feedback (with a small derivative gain because this shift of phase).

**Acknowledgements.** I would like to thank respectfully to Mr. Preumont, Professor and Director of Active Structure Laboratory from Free University of Brussels, Belgium. I worked a long time under his direction and I learned about many important theoretical and experimental procedures in dynamics.

## REFERENCES

Guan C., Zhang H., Hunt J.F., Yan H., *Determining Shear Modulus of thin Wood Composite Materials Using a Cantilever Beam Vibration Method*, Construction and Building Materials, **121**, 285-289 (2016).

Horodincă M., *A Study on Actuation Power Produced in an Active Damping System*, Mechanical Systems and Signal Processing, **39**, 1-2, 297-315 (2013).

Jassim Z.A., Ali N.N., Mustapha F., Abdul Jalil N.A., *A Review on the Vibration Analysis for a Damage Occurrence of a Cantilever Beam*, Engineering Failure Analysis, **31**, 442-461 (2013).

Kelly S.G, *Fundamentals of Mechanical Vibrations, Second Edition*, McGraw-Hill Series in Mechanical Engineering, ISBN 0-07-230092-2. (2000)

Kramer M.R., Zhanke L.,Young Y.L., *Free Vibration of Cantilevered Composite Plates in Air and in Water*, Composite Structures, **95**, 254-263 (2013).

Paimushin V.N., Firsov V.A., Günal I., Shishkin V.M., *Theoretical-Experimental Method for Determining the Material Damping Properties Based on the Damped Flexural Vibrations of Test Samples*, Procedia Engineering, **106**, 231-239 (2015).

*** https://www.mathworks.com/help/pde/examples/dynamics-of-a-damped-cantilever-beam.html (accessed on 30.09.2016).

## CERCETAREA EXPERIMENTALĂ A RĂSPUNSULUI LIBER PE PRIMUL MOD DE VIBRAŢIE (ÎNCOVOIERE) PENTRU O GRINDĂ ÎNCASTRATĂ LA UN CAPĂT

(Rezumat)

Lucrarea cercetează răspunsul liber pe primul mod de vibraţie flexională (încovoiere) pentru o grindă încastrată la un capăt, reflectat în semnalul furnizat de un sensor piezoelectric de tip plachetă, plasat prin lipire în proximitatea capătului încastrat al grinzii. Modelul teoretic general acceptat al acestui răspuns liber (amortizat vâscos, cu valori constante pentru gradul de amortizare şi pulsaţia proprie neamortizată) este contrazis, variaţii importante ale acestor parametri, ambii depinzând de amplitudinea vibraţiei. Cercetările au fost efectuate pe un stand experimental simplu (grindă încastrată la un capăt, senzor, osciloscop numeric şi calculator), cu aplicarea unor tehnici proprii de prelucrare asistată de calculator a semnalului furnizat de senzor.